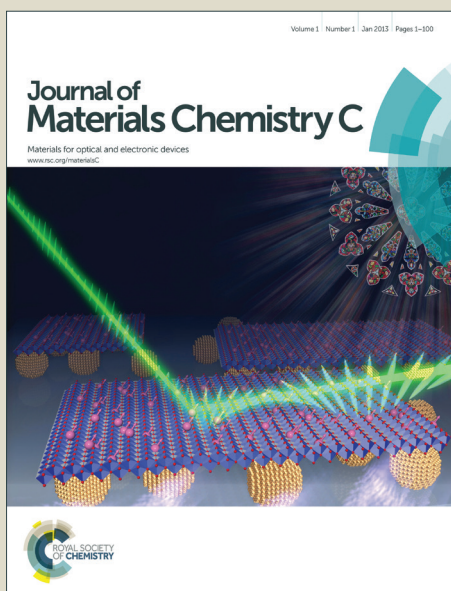


Journal of Materials Chemistry C

Accepted Manuscript



This is an *Accepted Manuscript*, which has been through the Royal Society of Chemistry peer review process and has been accepted for publication.

Accepted Manuscripts are published online shortly after acceptance, before technical editing, formatting and proof reading. Using this free service, authors can make their results available to the community, in citable form, before we publish the edited article. We will replace this *Accepted Manuscript* with the edited and formatted *Advance Article* as soon as it is available.

You can find more information about *Accepted Manuscripts* in the [Information for Authors](#).

Please note that technical editing may introduce minor changes to the text and/or graphics, which may alter content. The journal's standard [Terms & Conditions](#) and the [Ethical guidelines](#) still apply. In no event shall the Royal Society of Chemistry be held responsible for any errors or omissions in this *Accepted Manuscript* or any consequences arising from the use of any information it contains.

Synthesis and Optical Nonlinear Property of Novel Y-shaped Chromophores with Excellent Electro-Optic Activity

Cite this: DOI: 10.1039/x0xx00000x

Received 00th Sep 2015
Accepted 00th Sep 2015

DOI: 10.1039/x0xx00000x

www.rsc.org/

Yuhui Yang^{ab}, Hongyan Xiao^a, Haoran Wang^{ab}, Fenggang Liu^{ab}, Shuhui Bo^{*a},
Jialei Liu^a, Ling Qiu^a, Zhen Zhen^a, Xinhou Liu^{*a}

A series of Y-shaped chromophores A1, A2, B1 and B2 based on the same thiophene π -conjugation and tricyanofuran acceptor (TCF) but with different donors (modified phenothiazine and Triphenylamine) have been synthesized and systematically investigated in this paper. Density functional theory (DFT) was used to calculate the HOMO–LUMO energy gaps and first-order hyperpolarizability (β) of these chromophores. These chromophores showed excellent thermal stability with their decomposition temperatures all above 270 °C. Most importantly, the high molecular hyperpolarizability of these chromophores can be effectively translated into large electro-optic (EO) coefficients (r_{33}) in poled polymers. The doped films-C containing 25wt % chromophore B1 displayed an r_{33} value of 72 pm/V at 1310 nm, and the doped films-D containing B2 showed a value of 95 pm/V at the concentration of 25 wt %. These values are all much higher than the traditional FTC chromophore (39 pm/V). High r_{33} values indicated that the special Y structure can reduce intermolecular electrostatic interactions thus enhance the macroscopic EO activity. These properties, together with the good solubility, suggest the potential use of these new chromophores as advanced materials devices.

1. Introduction

Recently, high-performance organic electro-optic (EO) materials have been the focal point of research among many organic materials research groups. This research is driven by the attractive potential of improving the efficiency of nonlinear optical (NLO) material while lowering production cost for applications in telecommunications, optical modulation and optical memory.¹⁻⁴ Over the past two decades, the NLO materials have drawn considerable attention and have stimulated a research boom for materials with large EO activities, both at molecular level (β) and as processed materials (r_{33}).^{2, 5-7} In recent years, NLO chromophores with large values of hyperpolarizabilities (β) have been developed. However, efficient arrangement of NLO chromophores has proven challenging. Organic NLO chromophores, especially those demonstrating high hyperpolarizability (β) values, typically have large ground state dipole moment, tend to lower the NLO response at higher chromophore loading levels due to aggregation effects. So for practical applications, one of the often encountered challenges in making highly efficient EO materials is to develop nonlinear optical (NLO) chromophores with large hyperpolarizabilities (β) and to reduce adverse strong inter-molecular electrostatic interaction among the

chromophores molecules also with excellent thermal stabilities.⁸⁻¹⁰ As a result, careful design of chromophores and control of the assembly and lattice hardening in a proper polymer matrix is needed.¹¹

Poled polymers are the most widely studied organic NLO materials. The macroscopic NLO response of such materials arises from the poling-induced polar order of noncentrosymmetric NLO chromophores in polymers.⁷ In general, the second-order NLO chromophore can be divided into three blocks: electro-donor, π -conjugated bridge and strong electro-acceptor, called D- π -A system.¹² When under an applied external electric field, the donor and acceptor substituents can provide the requisite ground-state charge asymmetry, whereas the π -conjugation bridge provides a pathway for the ultrafast redistribution of electric charges. Unfortunately, in most of the poled polymers, the chromophore moieties which have a rod-like structure and the strong dipole-dipole interactions between chromophores have led to unfavorable antiparallel packing of the chromophores, making the conversion from the high β values of the chromophores to large macroscopic optical nonlinearities (r_{33}) a continual challenge.^{13, 14} So the most effective and facile way to improve the r_{33} values of the guest-host EO materials is the optimization of the push-pull chromophores.

ARTICLE

Alex K.Y. Jen et al. have done much effort in the molecular modification to optimize the NLO properties with large r_{33} values.^{1,15,16} As it said, controlling the shape of the chromophore was proven to be an efficient approach for minimizing this interaction and enhancing the poling efficiency. In this paper, we designed a series of Y-shaped chromophores. The special Y structure is different from the general NLO chromophores showing the rod-like structure, which may have an obvious advantage in translating β into r_{33} values and thus increased the macroscopic EO activity. To the best of our knowledge, the Y-shaped chromophore rarely appeared in NLO chromophore before.

Considering the mentioned advantages above, so in this paper, we had designed and synthesized a series of Y-shaped chromophores containing an identical TCF acceptor, but with different electron donors (modified phenothiazine and Triphenylamine). These new chromophores (in chart 1) showed great solubility in common organic solvents, good compatibility with polymers, and large EO activity in the poled films. ¹H-NMR and ¹³C-NMR analysis were carried out to demonstrate the preparation of these chromophores. Thermal stability, photophysical properties, DFT calculations and EO activities of these chromophores were systematically studied compared to the traditional rod-like chromophore FTC.

2. Results and discussion

2.1 Synthesis and characterization of chromophores

Synthesis of A1, B1, A2 and B2 chromophores were depicted in scheme 1, scheme 2, respectively. The difference between chromophore A1 and B1 was the length of the π -bridge. Chromophore B1 was obtained in seven steps starting from the commercially available phenothiazine (Scheme 1). Compound 3a was synthesized according to the literature.¹⁷ The compounds 4a were synthesized by the Ullmann reaction from 3a using the powerful catalytic system about the combination of Pd(dba)₂ and HP(t-Bu)₃BF₄. The reduction with DIBAL-H followed by acid hydrolysis converts the nitrile group on 4a into the corresponding aldehyde 5a with 82% yield. The target chromophore A1 was obtained via Knoevenagel condensation reaction of the aldehyde 5a with acceptor TCF in the presence of a catalytic amount of triethylamine. On the other hand, the aldehyde 5a was condensed with 2-thienyltriphenylphosphonate bromide by Wittig condensation to gain 6a. As expected, after introduction of the thiophene bridge by Wittig condensation, treatment of compound 6a with n-BuLi and DMF gave an aldehyde 7a. The target chromophore B1 was obtained via Knoevenagel condensation reaction of the aldehyde 7a with

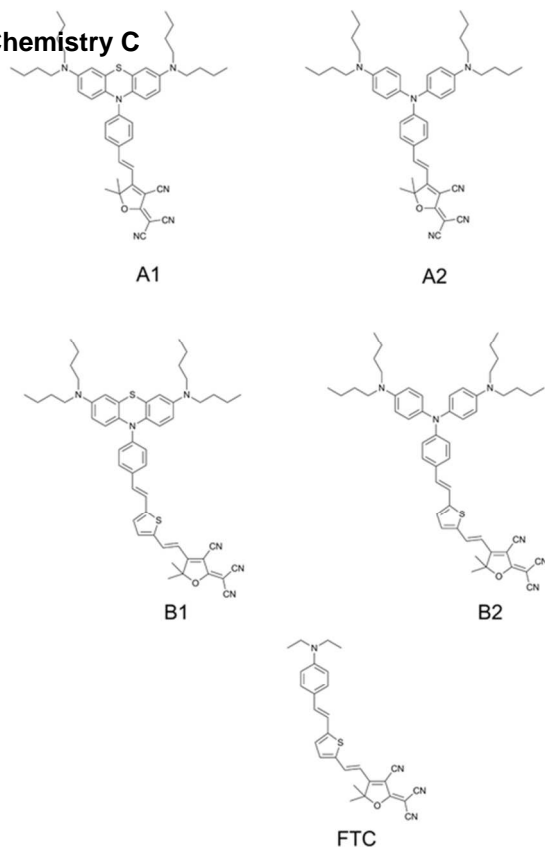
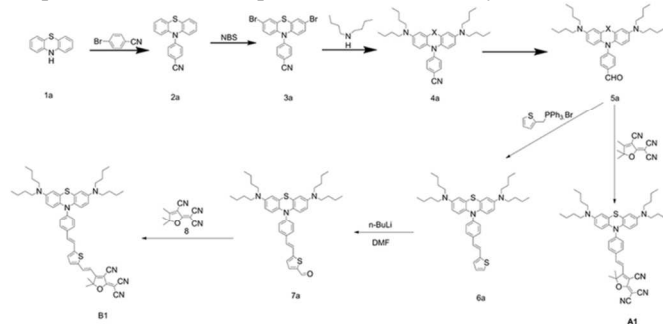


Chart 1 the structure of the chromophores A1, A2, B1, B2 and FTC

acceptor TCF in the presence of a catalytic amount of

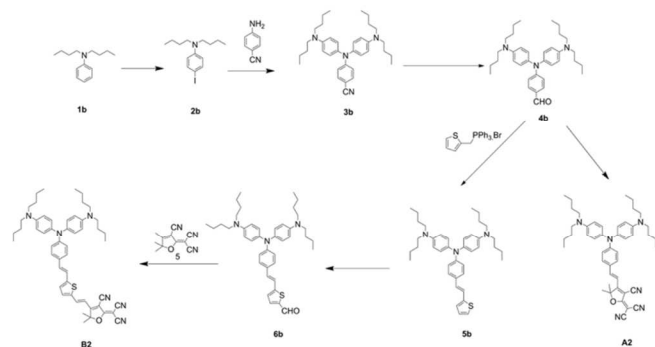


Scheme 1 Chemical structures and synthetic scheme for chromophore A1 and B1

triethylamine. The chromophore A2 and B2 were synthesized according to the literature.¹⁸ All of the chromophores were fully characterized by ¹H-NMR, ¹³C-NMR, and mass spectroscopy. These chromophores possess good solubility in common organic solvents, such as dichloromethane, chloromethane and acetone.

2.2 Thermal analysis

NLO chromophores must be thermally stable enough to withstand encountered high temperatures ($>200\text{ }^{\circ}\text{C}$) in electric field poling and subsequent processing of



Scheme 2 Chemical structures and synthetic scheme for chromophore A2 and B2

chromophore/polymer materials. Thermal properties of these chromophores were measured by Thermogravimetric Analysis (TGA). As shown in figure 1 and table 1, the decomposition temperature (T_d) of chromophores A1, A2, B1 and B2 are all above $270\text{ }^{\circ}\text{C}$, which are much higher than the traditional FTC chromophore ($242\text{ }^{\circ}\text{C}$)¹⁹. These data indicate that the special Y structure can increase the thermal stability of the chromophore.

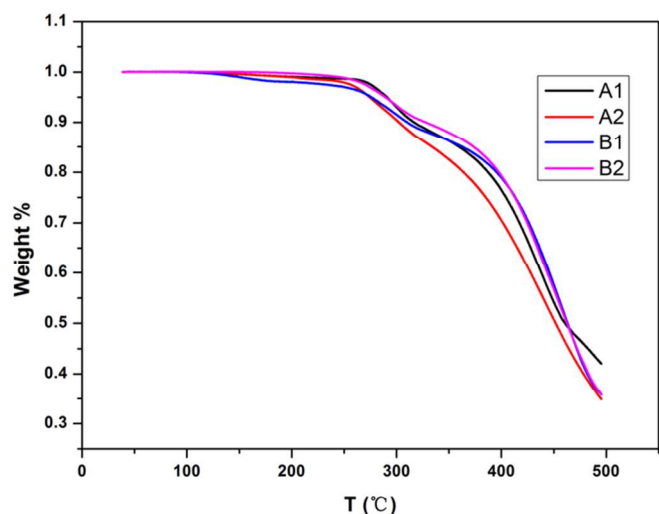


Figure 1 TGA curves of chromophores A1, A2, B1 and B2 with a heating rate of $10\text{ }^{\circ}\text{C min}^{-1}$ in nitrogen atmosphere

All of these novel Y-shaped chromophores showed excellent stability and the T_d of these novel chromophores was high enough for the application in EO device preparation.

2.3 Optical properties

In order to reveal the effect of the Y-shaped structure on the intramolecular charge transfer (ICT) of dipolar chromophores, UV-Vis absorption spectra of these chromophores ($c=1\times 10^{-5}\text{ mol/L}$) were measured in a series of aprotic solvents with different polarity so that the solvatochromic behavior of these chromophores could be investigated to explore the polarity of chromophores in a wide range of dielectric environments (Figure 2). The spectrum data are summarized in Table 1. The synthesized chromophores exhibited a similar $\pi\rightarrow\pi^*$ intramolecular charge-transfer (ICT) absorption band in the visible region. A1 shows a maximum absorption (λ_{max}) of 599 nm . By extending the π -bridge of the chromophore A1, the λ_{max}

of B1 was red shifted by 60 nm to 659 nm . The difference between the chromophore B1 and B2 is the donor group. Compared with the chromophore B1, the λ_{max} of the chromophore B2 was red shifted by 71 nm to 730 nm .¹⁸ This result indicated that the modified triarylamino-phenyl-based donor shifted the ICT absorption band of the chromophore to a lower energy. As shown in Figure 2, the peak wavelength of A1, A2, B1 and B2 showed a bathochromic shift of $52, 69, 49$ and 72 nm from dioxane to chloroform respectively. As reported¹⁹, the traditional FTC showed a bathochromic shift of 55 nm . Chromophore A2, B2 displayed the larger solvatochromism compared with the traditional FTC chromophore. These results implied that these new Y-shaped chromophores were more easily polarizable than the traditional FTC chromophore. Besides, Chromophore A2, B2 displayed the larger solvatochromism compared with the A1 and B1, which confirmed that the modified triarylamino-phenyl-based chromophore was more easily polarizable than the chromophore with the modified phenothiazine. These analyses implied that sulfur atom linking the two Benzenes rings on the donor part may weaken the electron-donating.

Table 1. Summary of Thermal and Optical Properties and EO Coefficients of Chromophores A1-B2 and FTC

Chromophore	T_d^a ($^{\circ}\text{C}$)	λ_{max}^b (nm)	λ_{max}^c (nm)	$\Delta\lambda^d$ (nm)	r_{33}^e (pm/V)
A1	291	599	547	52	33
A2	276	659	590	69	47
B1	274	659	610	49	78
B2	289	730	658	72	95
FTC	242	676	621	55	30

^a T_d was determined by an onset point, and measured by TGA under nitrogen at a heating rate of $10\text{ }^{\circ}\text{C min}^{-1}$.

^b λ_{max} was measured in CHCl_3 , ^c λ_{max} was measured in dioxane.

^d $\Delta\lambda = \lambda_{\text{max}}^b - \lambda_{\text{max}}^c$

^e r_{33} values were measured at the wavelength of 1310 nm .

2.4 Theoretical calculations

To understand the ground-state polarization and microscopic NLO properties of the designed chromophores, the DFT calculations were carried out at the B3LYP level by employing the split valence 6-31 G* (d, p) basis set using the Gaussian 09 program package.²⁰⁻²² The first hyperpolarizability (β) values were calculated at CAM-B3LYP level by employing 6-31G* basis set using the Gaussian 09 and the direction of the maximum value is directed along the charge transfer axis of the chromophores. The data obtained from DFT calculations are summarized in Table 2.

The frontier molecular orbitals are often used to characterize the chemical reactivity and kinetic stability of a molecule and to obtain qualitative information about the optical and electrical properties of molecules.^{22, 23, 24} Besides, the HOMO-LUMO energy gap is also used to understand the charge transfer interaction occurring in the chromophore molecule.²⁴⁻²⁶ In the case of these chromophores, Figure 3 represents the frontier molecular orbitals of chromophores A1, A2, B1 and B2. According to the Figure 3, it is clear that the electronic

distribution of the HOMO is delocalized over the donor and π -bridge part, whereas the LUMO is mainly constituted by the acceptor moieties.²⁴

The HOMO and LUMO energy were calculated by DFT calculations as shown in Figure 3 and Table 2. In view of chromophore A1 and A2, chromophore A2 narrows the energy gap between the HOMO and LUMO energy with ΔE values of

2.17 eV. By contrast, the ΔE value of A1 is 2.39 eV. When extended the π -bridge of chromophore A1 and A2 to chromophore B1 and B2 respectively, we can find similar results of chromophore B2 narrows the energy gap between the

Table 2. Data from DFT calculations

Chromophores	E_{HOMO} /eV	E_{LUMO} /eV	ΔE^a /eV	β_{max}^c /10 ⁻³⁰ esu
A1	-5.18	-2.79	2.39	329.90
A2	-4.98	-2.81	2.17	458.87
B1	-4.92	-3.06	1.86	962.94
B2	-4.97	-3.29	1.68	1561.80

^a $\Delta E = E_{\text{LUMO}} - E_{\text{HOMO}}$

^bResults was calculated by DFT

^cResults was from cyclic voltammetry experiment

^d β values were calculated using gaussian 09 at CAM-B3LYP/6-31+G* level

and the direction of the maximum value is directed along the charge transfer

axis of the chromophores.

HOMO and LUMO energy with ΔE values of 1.68 eV. The HOMO–LUMO gaps of chromophore B2 (1.68 eV) is lowest and A1 (2.39 eV) is the largest. This result indicates that chromophore B2 may exhibit better ICT and NLO property than B1. As reported²⁴, the optical gap is lower, the charge-transfer (ICT) ability is greater and thus improve the nonlinearity. Chromophores A2 and B2 showed a lower optical gap, so it indicated that B2 may exhibit better ICT and NLO property than B1 chromophore. Meanwhile, chromophore A2 may exhibit better ICT and NLO property than A1. This result corresponded with the conclusion of UV-Vis spectra analysis.

Further, the theoretical microscopic β was calculated by Gaussian 09. The β value is related to the substituent, molecular configuration, and intramolecular charge-transfer. As the reference reported earlier, the β has been calculated at CAM-B3LYP/6-31G* level.²⁷ From this, the scalar quantity of β can be computed from the x, y, and z components according following equation.

$$\beta = (\beta_x^2 + \beta_y^2 + \beta_z^2)^{1/2} \quad (1)$$

Where $\beta_i = \beta_{ii} + \frac{1}{3} \sum_{j \neq i} (\beta_{ij} + \beta_{ji} + \beta_{ji})$, $i, j \in (x, y, z)$

Due to the extended π -bridge, chromophores B series showed a larger β value than A series chromophores. Besides, due to the stronger electron-donating ability and better conjugated system (Figure 4), chromophore B2 showed much larger β value than the B1 chromophore. (962.94×10^{-30} vs 1057.3×10^{-30} esu). This result is well corresponded with the conclusion of UV-Vis spectra analysis.

To understand the influence of the heteroatom on donor part deeply, the composition of the HOMOs and LUMOs were calculated using the Multiwfn program with Ros-Schuit (SCPA) partition.²⁸ As shown in Table 3, the chromophores A1, A2, B1 and B2 were segmented as donor, π -bridge, and acceptor. At the same time, the attributions of the sulfur atom and nitrogen atoms located in donor moiety were listed separately. For the chromophores A1, A2, B1 and B2, the HOMO was largely stabilized by the contributions from donor (85.64%, 88.29%,

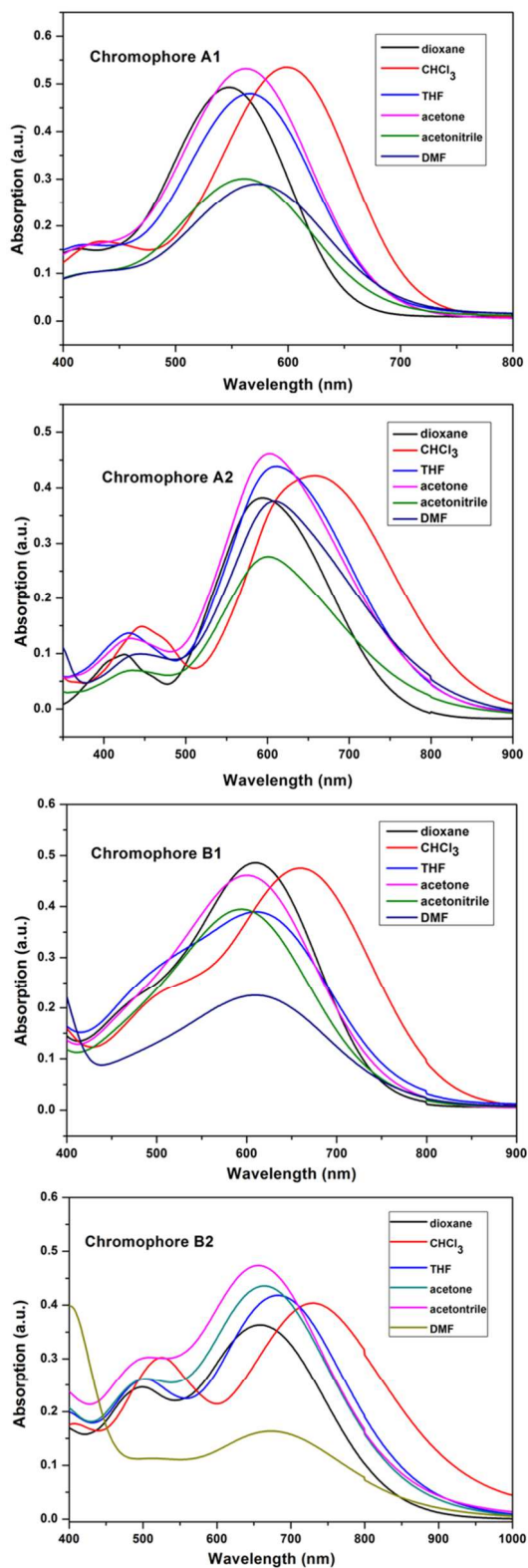


Figure 2 UV-Vis absorption spectra in different solvents of chromophore A1, A2, B1 and B2 ($c = 1 \times 10^{-5}$ mol L⁻¹)

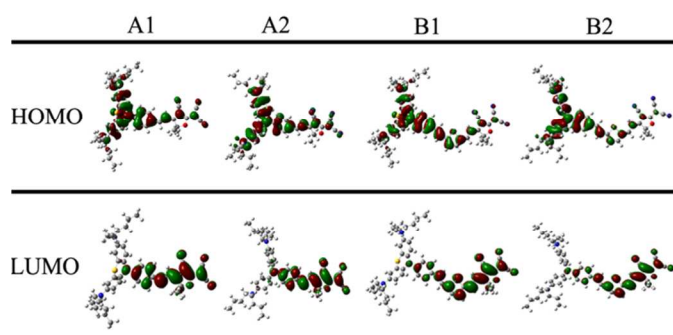


Figure 3 The frontier molecular orbitals of chromophores A1, A2, B1 and B2 (76.49% and 84.37%) and much less contributions from other segments. As the difference between the A1, A2 and B1 and B2 is similar, we only discussed the chromophore B1 and B2 in detail. For chromophore B1, the contribution of the π -bridge was 15.06% and 39.95% to the HOMO and LUMO level respectively. For the chromophore B2, the contribution of π -bridge was 10.34% and 39.60% to the HOMO and LUMO level respectively. However, the contributions of the three nitrogen-atoms located in donor moiety to the HOMO of the chromophores were obviously different. The contribution to the HOMO level was 27.33% from chromophore B1, but the contribution was 31.22% for chromophore B2. Besides, the contribution of the sulfur atom located in donor moiety to the HOMO of the chromophore B1 was 2.10%. This result indicated that the sulfur atom linked the two benzenes rings together showed a much weaker donatability and the sulfur atom led to the donor ability of three nitrogen-atoms weakened. This can be explained in the figure 5, the angle between the double benzenes rings is 131.59° and 83.0° for chromophores B1 and B2 respectively. The sulfur atom linked the two benzenes ring together made the angle between two benzenes ring much larger and thus weakened the donor ability. This result corresponded with the UV-Vis analysis and DFT results.

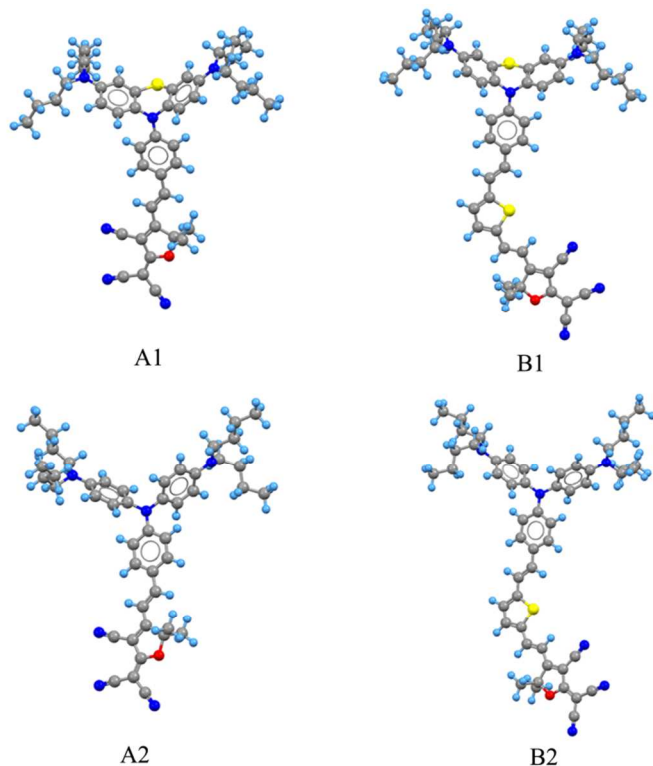


Figure 4 The optimized structure of chromophore A1, A2, B1 and B2

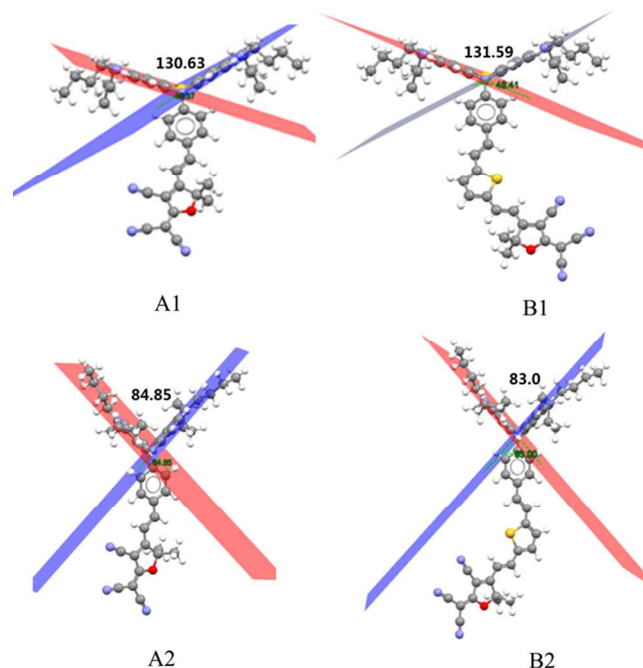


Figure 5 The angles between the two benzenes

2.5 Electric field poling and EO property measurements.

For studying EO property derived from these chromophores, a series of guest-host polymers were generated by formulating the chromophores into amorphous polycarbonate (APC) using dibromomethane as solvent. The resulting solutions were filtered through a $0.2\text{-}\mu\text{m}$ PTFE filter and spin-coated onto indium tin oxide (ITO) glass substrates. Films of doped polymers were baked in a vacuum oven at 80°C overnight to ensure the removal of the residual solvent. The corona poling process was carried out at a temperature of 10°C above the glass transition temperature (T_g) of the polymer. The r_{33} values were measured using the Teng-Man simple reflection technique at the wavelength of 1310 nm using a carefully selected thin ITO electrode with low reflectivity and good transparency in order to minimize the contribution from multiple reflections.²⁹ As reported earlier,³⁰⁻³⁴ the introduction of some isolation groups into the chromophore moieties to further control the shape of the chromophore could be an efficient approach to minimize interactions between the chromophores, so these new Y-shaped chromophores may have an obvious advantage in translating β values into r_{33} values and thus increased the macroscopic EO activity.

The EO coefficient (r_{33}), defining the efficiency of translating molecular microscopic hyperpolarizability into macroscopic EO activities, was described as follows:

$$r_{33} = 2N f(\omega) \beta \langle \cos^3 \theta \rangle / n^4 \quad (2)$$

Where r_{33} is the EO coefficient of the poled polymer, N represents the aligned chromophore number density and $f(\omega)$ denotes the Lorentz-Onsager local field factors. The term $\langle \cos^3 \theta \rangle$ is the orientationally averaged acentric order parameter characterizing the degree of noncentrosymmetric alignment of the chromophore in the material and n represents the refractive index.⁵ Before poling, there is no EO activity in the EO material and the chromophores in material are thermal randomization. Electrical field induced poling was proceeded to induce the acentric ordering of chromophores. Realization of

Table 3 Molecular orbital composition (%) in the ground state for chromophores A1, A2, B1 and B2.

	A1		A2		B1		B2	
	HOMO (%)	LUMO (%)						
D	85.64	43.23	88.29	44.67	76.49	15.23	84.37	16.22
π	4.49	2.45	3.87	2.61	15.06	39.95	10.34	39.60
A	9.87	54.32	7.84	52.72	8.45	44.82	5.29	4.18
^a N	31.79	4.16	32.97	4.36	27.33	15.58	31.22	1.82
^b S	2.58	0.11	---	---	2.10	0.04	---	---

^aN the three nitrogen atoms located on the donor part

^bS the sulfur atom located on the donor part of the chromophores A1 and B1

large electro-optic activity for dipolar organic chromophore-containing materials requires the simultaneous optimization of chromophore first hyperpolarizability (β), acentric order $\langle \cos^3\theta \rangle$, and number density (N).^{36, 37} When at low concentration, the electro-optic activity increased with chromophore density, dipole moment and the strength of the electric poling field. However, when the concentrations of chromophores increased to a certain extent, the N and $\langle \cos^3\theta \rangle$ are no longer independent factors. Then

$$\langle \cos^3\theta \rangle = (\mu F / 5kT) [1 - L^2(W/kT)] \quad (3)$$

Where k is the Boltzmann constant and T is the Kelvin (poling temperature). $F = [f(0)E_p]$ where E_p is the electric poling field. L is the Langevin function, which is a function of W/kT , the ratio of the intermolecular electrostatic energy (W) to the thermal energy (kT). L is related to electrostatic interactions between molecules. So when the intermolecular electrostatic interactions are neglected, the electro-optic coefficient (r_{33}) should increase linearly with chromophore density, dipole moment, first hyperpolarizability and the strength of the electric poling field.

The r_{33} values of films containing chromophores A1 (film-A), A2 (film-B), B1 (film-C) and B2 (film-D) were measured in different loading densities, as shown in table 4 and Figure 6. For chromophore A1, the r_{33} values were gradually improved from 9 pm V^{-1} (10 wt%) to 31 pm V^{-1} (25 wt%), as the concentration of chromophores increased, the similar trend of enhancement was also observed for chromophore A2, whose r_{33} values increased from 13 pm V^{-1} (10 wt%) to 47 pm V^{-1} (25 wt%). Film-C containing chromophore B1 gained the r_{33} values from 22 pm V^{-1} (10 wt%) to 72 pm V^{-1} (25 wt%) and the similar trend of enhancement was also observed for chromophore B2, whose r_{33} values increased from 28 pm V^{-1} (10 wt%) to 95 pm V^{-1} (25 wt%).¹⁸ However, as reported before¹⁹, the traditional rod-like FTC chromophore, whose r_{33} values only increased from 12 pm V^{-1} (10 wt%) to 39 pm V^{-1} . To our regret, when the chromophore loading density was increased to 30 wt%, all of these films presented a downtrend.

Through the outcome above, we can obviously see that the chromophore B1 have nearly 2 times higher r_{33} value than the chromophore FTC and chromophore B2 have nearly 3 times higher r_{33} value than the chromophore FTC, illustrating that

these novel Y-shaped structures significantly increase their macroscopic EO activity. Besides, from the figure 6, we can see

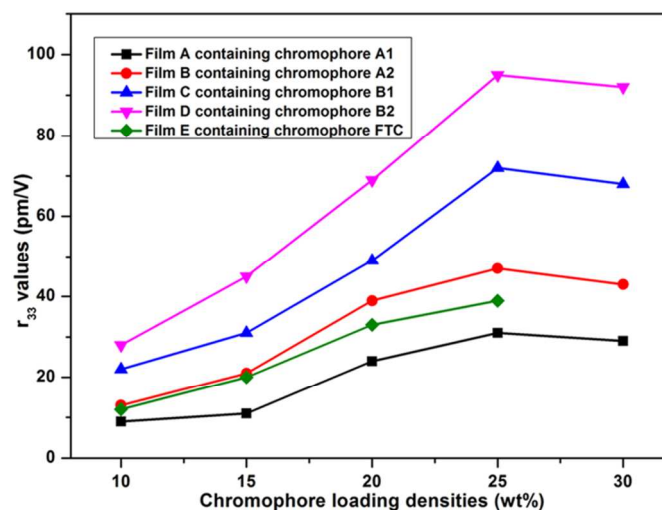


Figure 6 EO coefficients of NLO thin films as a function of chromophore loading densities

that the film-D containing chromophore B2 showed higher r_{33} values than the film-C containing the chromophore B1, which illustrating that the increased donor strength of the chromophores significantly increase their macroscopic EO activities. This result can be explained as follows: When the concentration of chromophore in APC is low, the intermolecular dipolar interactions are relatively weak. The film-D/APC achieved the largest r_{33} value probably due to its largest β and good polarizability. With relatively low β , the r_{33} value of film-C/APC was smaller than that of film-D/APC. The drop in EO activity from film-B/APC to film-A/APC is mainly associated with the lowest β of chromophore A1 in the polar polymer matrix and the inefficient poling, because of its lower polarizability than the other chromophores.

As the chromophore loading densities increased, the effect of inter-chromophore dipole-dipole interaction is becoming stronger. As results showed, these r_{33} values are almost higher than the traditional FTC chromophores ($r_{33}=39 \text{ pm/V}$).¹⁹ This result proved that these novel Y-shaped chromophores have an

Table 4 Summary of EO Coefficients of Chromophores A1-B2 and FTC at different densities

Wt%	ϵ_{33} (pm/V)				
	A1	A2	B1	B2	FTC
10	9	13	22	28	12
15	11	21	31	45	20
20	24	39	49	69	33
25	31	47	72	95	39
30	29	43	68	92	--

^a ϵ_{33} values were measured at the wavelength of 1310nm.

obvious advantage in reducing intermolecular electrostatic interactions thus enhance the macroscopic EO activity.

3. Experimental

3.1 Materials and instrumentation

¹H NMR spectra were determined by an Advance Bruker 400(400 MHz) NMR spectrometer (tetramethylsilane as internal reference). The MS spectra were obtained on MALDI-TOF-(Matrix Assisted Laser Desorption/Ionization of Flight) on BIFLEXIII(Broker Inc.) spectrometer. The UV-Vis spectra were performed on Cary 5000 photo spectrometer. The TGA was determined by TA5000-2950TGA (TA Co) with a heating rate of 10 °C / min under the protection of nitrogen. All chemicals, commercially available, are used without further purification unless stated. The DMF, toluene, 1, 4-dioxane and THF were freshly distilled prior to its use. The 2-dicyanomethylene-3-cyano-4-methyl-2, 5-dihydrofuran (TCF) acceptor was prepared according to the literature.³⁵

3.2 Synthesis

3.2.1 Compound 2a and 3a was synthesized according to the literature.¹⁷

3.2.2 Synthesis of compound 4a

In a dry Schlenk tube and under nitrogen, compound 3a (4.58 g, 0.01 mol), Pd(dba)₂ (0.274 g, 0.03 mol), HP(t-Bu)₃BF₄ (0.145 g, 0.1 mol), and NaOtBu (2.88 g, 0.03 mol) were dissolved in dry 1,4-dioxane (60 mL). The reaction mixture was stirred at 70 °C for 5 minutes and then the dibutylaminee (2.85 g, 0.11 mol) was added under nitrogen and the mixture was heated to 110 °C for 24 h. After cooling to room temperature, the reaction mixture was diluted with ethyl acetate. The organic layer was dried over MgSO₄ and evaporated. The residue was purified by column chromatography on silica gel (hexane/acetone, v/v, 50:1). Yellow oil was obtained (3.36 g, 61%).

¹H NMR (400 MHz, CDCl₃) δ 7.34 (d, J = 8.6 Hz, 2H), 7.25 (d, J = 8.7 Hz, 2H), 6.93 (d, J = 8.6 Hz, 2H), 6.68 (s, 2H), 6.57 (d, J = 8.7 Hz, 2H), 3.32 – 3.17 (m, 8H), 1.63 – 1.49 (m, 8H), 1.41 – 1.28 (m, 8H), 1.03 – 0.90 (m, 12H).

¹³C NMR (100 MHz, CDCl₃) δ 152.05, 146.67, 136.23, 133.10, 129.19, 128.15, 120.41, 113.24, 110.98, 110.29, 100.49, 50.98, 29.34, 20.35, 14.02.

MALDI-TOF: m/z calcd for C₃₅H₄₆N₄S:754.34[M]⁺; found: 554.25.

3.2.3 Synthesis of compound 5a

To a solution of 4a (3.32 g, 6 mmol) in dry toluene (50 mL) was added a 1 M solution of diisobutylaluminum hydride in hexanes (12 mL, 12 mmol) by syringe at -78 °C with a dry ice/acetone bath. The reaction was stirred at -78 °C for 2 h. After the mixture was warmed to room temperature, NH₄Cl solution was added to quench the reaction. The mixture was stirred for 1h to complete the hydrolysis. The organic solvent was collected and removed in vacuo. The residue was purified by column chromatography on silica gel (hexane/acetone, v/v, 10/1) to yield red oil (2.74 g, 82%).

¹H NMR (400 MHz, Acetone) δ 9.59 (s, 1H), 7.47 (d, J = 8.9 Hz, 2H), 7.18 (d, J = 8.8 Hz, 2H), 6.85 (d, J = 8.9 Hz, 2H), 6.62 (d, J = 2.8 Hz, 2H), 6.55 (dd, J = 8.8, 2.8 Hz, 2H), 3.15 (m, 8H), 1.42 (m, 8H), 1.28 – 1.13 (m, 8H), 0.79 (m, 12H).

¹³C NMR (100 MHz, Acetone) δ 204.95, 189.30, 153.55, 146.73, 136.11, 130.99, 129.40, 128.39, 128.25, 50.61, 20.09, 13.58.

MALDI-TOF: m/z calcd for C₃₅H₄₇N₃OS:557.34 [M]⁺; found: 557.31.

3.2.4 Synthesis of compound A1

A mixture of compound 5a (0.557 g, 1.00 mmol) and acceptor TCF (0.22 g, 1.10 mmol) in chloroform (30 mL) was stirred at 65 °C for 4 h in the presence of a catalytic amount of triethylamine. After removal of the solvent, the residue was purified by column chromatography on silica gel (hexane/acetone, v/v, 6:1). A dark solid was obtained (0.28 g, 38%).

¹H NMR (400 MHz, Acetone) δ 7.95 (d, J = 16.3 Hz, 1H), 7.72 (d, J=8.2 Hz 2H), 7.36 (d, J = 8.2 Hz, 2H), 7.03 (m, 4H), 6.80 (s, 1H), 6.76 (m, 3H), 3.38 (m, 8H), 1.64 (m, 8H), 1.40 (m, 8H), 0.97 (m, 12H).

¹³C NMR (100 MHz, Acetone) δ 176.93, 176.54, 175.46, 174.38, 152.64, 148.13, 147.10, 139.76, 138.50, 137.43, 131.60, 128.03, 127.75, 125.66, 117.62, 112.60, 111.74, 110.71, 54.95, 50.71, 25.42, 20.14, 13.46.

MALDI-TOF: m/z calcd for C₄₆H₅₄N₆OS:738.41 [M]⁺; found: 738.13.

3.2.5 Synthesis of compound 6a

Under N₂, to a mixture of compound 5a (1.12 g, 2 mmol) and 2-thienyl triphenylphosphonate bromide (0.97 g, 2.2 mmol) in dry THF (20 mL) at room temperature, NaH (0.48 g, 0.02 mol) was added. The mixture turned yellow and was stirred at room temperature for 24 h. Saturated NH₄Cl was added and the resulting mixture was extracted with EtOAc (20×3 mL). The combined extracts were washed with water and dried over MgSO₄. After filtration and removal of the solvent under vacuum, the residue was purified by column chromatography on silica gel (hexane/acetone, v/v, 10/1) to obtain a yellow liquid (0.99 g, 78%).

¹H NMR (400 MHz, Acetone) δ 7.51 (d, J = 8.6 Hz, 2H), 7.31 (d, J = 3.1 Hz, 1H), 7.29 (d, J = 8.6 Hz, 2H), 7.11 (d, J=11.6Hz, 1H), 7.09 (m, 1H), 7.04 (d, J = 3.1 Hz, 1H), 6.85 (d, J = 8.9 Hz, 2H), 6.62 (s, 2H), 6.55 (d, J = 8.8, 2H), 6.43 (d, J = 11.6 Hz,

1H), 3.15 (m, 8H), 1.42 (m, 8H), 1.28 – 1.13 (m, 8H), 0.79 (m, 12H).

MALDI-TOF: m/z calcd for C₄₀H₅₁N₃OS₂:637.35 [M]⁺; found: 637.23.

3.2.6 Synthesis of compound 7a

To a solution of compound 6a (0.99 g, 1.55 mmol) in dry THF (20 mL) a 2.4 M solution of n-BuLi in hexane (1 mL, 2.30 mmol) was added dropwise at -78 °C under N₂. After this mixture was stirred at this temperature for 1 h, dry DMF (0.2 mL, 1.86 mmol) was introduced. The resulting solution was stirred for another 1h at -78 °C and then allowed to warm up to room temperature. The reaction was quenched by water. THF was removed by evaporation. The residue was extracted using CH₂Cl₂ (3 × 30 mL). The organic layer was dried by MgSO₄ and concentrated in vacuo. The residue was purified by column chromatography on silica gel (hexane/acetone, v/v, 10/1) to obtain a red liquid (0.80 g, 78%).

¹H NMR (400 MHz, Acetone) δ 9.88 (s, 1H), 7.84 (d, J = 3.9 Hz, 1H), 7.43 (d, J = 8.8 Hz, 2H), 7.29 – 7.21 (m, 5H), 6.93 (d, J = 8.8 Hz, 2H), 6.77 – 6.69 (m, 4H), 3.36 (m, 8H), 1.62 (m, 8H), 1.41 (m, 8H), 0.97 (m, 12H).

¹³C NMR (100 MHz, Acetone) δ 182.38, 152.95, 146.42, 140.91, 137.95, 135.21, 132.80, 130.51, 127.89, 127.28, 125.99, 117.44, 114.68, 110.63, 110.47, 50.58, 20.03, 13.37.

MALDI-TOF: m/z calcd for C₄₁H₅₁N₃OS₂:665.35 [M]⁺; found: 665.21.

3.2.7 Synthesis of chromophore B1

A mixture of aldehydic bridge 7a (0.67 g, 1 mmol) and acceptor 6 (0.22 g, 1.10 mmol) in chloroform (30 mL) was stirred at 62 °C for 4 h in the presence of a catalytic amount of triethylamine. After removal of the solvent, the residue was purified by column chromatography on silica gel (hexane/acetone, v/v, 5:1). A dark solid was obtained (0.31 g, 37%).

¹H NMR (400 MHz, Acetone) δ 8.16 (d, J = 15.9 Hz, 1H), 7.68 (d, J = 4.0 Hz, 1H), 7.46 (d, J = 8.7 Hz, 2H), 7.34 – 7.19 (m, 5H), 6.92 (m, 2H), 6.86 (d, J = 15.9 Hz, 1H), 6.75 (m, 4H), 3.46 – 3.30 (m, 8H), 1.90 (s, 6H), 1.63 (m, 8H), 1.42 (m, 8H), 1.03 – 0.92 (m, 12H).

¹³C NMR (100 MHz, Acetone) δ 176.49, 174.26, 152.61, 146.31, 139.67, 138.10, 137.45, 133.20, 131.01, 127.99, 127.35, 117.28, 112.66, 112.52, 111.41, 110.50, 98.14, 97.36, 60.43, 59.64, 25.33, 19.99, 13.39.

MALDI-TOF: m/z calcd for C₅₂H₅₈N₆OS₂:846.41 [M]⁺; found:846.26.

3.2.8 Compound 1b-4b, Chromophore B2 were synthesized according to the previous work.¹⁸

3.2.9 Synthesis of chromophore A2

In a similar manner described above, chromophore A2 was synthesized from 4b as dark solid (41%).

¹H NMR (400 MHz, Acetone) δ 7.95 (d, J = 16.0 Hz, 1H), 7.68 (d, J = 8.8 Hz, 2H), 7.12 – 7.03 (m, 4H), 6.97 (d, J = 16.0, 1H), 6.81 – 6.67 (m, 6H), 3.40 – 3.29 (m, 8H), 1.84 (s, 6H), 1.65 – 1.52 (m, 8H), 1.37 (m, 8H), 0.95 (m, 12H).

¹³C NMR (100 MHz, Acetone) δ 176.95, 175.13, 154.10, 148.37, 146.58, 133.23, 131.94, 127.98, 124.12, 116.18,

112.79, 112.40, 112.07, 111.40, 109.33, 97.79, 93.93, 52.89, 50.39, 25.37, 19.94, 13.26.

MALDI-TOF: m/z calcd for C₄₆H₅₆N₆O:708.45 [M]⁺; found: 708.72.

4. Conclusions

In this research, two series NLO chromophores based on the Y-shaped structure have been synthesized and systematically investigated by NMR, MS and UV-vis absorption spectra. The energy gap between ground state and excited state together with molecular nonlinearity were studied by UV-vis absorption spectroscopy, DFT calculations and EO measurements. Theoretical and experimental investigations suggest that by optimizing the structure of the chromophores can dramatically improve the nonlinear optical properties. These novel chromophores present Y shape with good thermal stability and large molecular hyperpolarizabilities, which can be effectively translated into very large EO coefficients in poled polymers. The doped film-D containing chromophore B2 displayed a maximum r₃₃ value of 95 pm/V at the doping concentration of 25 wt %, while film-C containing chromophore B1 showed a maximum r₃₃ value of 72 pm/V at 25 wt %. Those consequences indicate that the special Y structure could efficiently reduce the interchromophore electrostatic interactions and enhance the macroscopic optical nonlinearity. These novel Y-shaped chromophores showed promising applications in NLO chromophore synthesis. We believe that these novel Y-shaped chromophores can be used in exploring high-performance organic EO and photorefractive materials where both thermal stability and optical nonlinearity are of equal importance.

Acknowledgements

All calculations were performed on the cluster of Key Laboratory of Theoretical and Computational Photochemistry, Ministry of Education, China. We are grateful to the National Nature Science Foundation of China (no.61101054 and no. 21003143) for financial support.

Notes and references

a Key Laboratory of Photochemical Conversion and Optoelectronic Materials, Technical Institute of Physics and Chemistry, Chinese Academy of Sciences, Beijing 100190, PR China

b University of Chinese Academy of Sciences, Beijing 100043, PR China

* Corresponding authors. Tel.: +86-01-82543528; Fax: +86-01-62554670.

E-mail address: boshuhui@mail.ipc.ac.cn (S. Bo) and xinhoului@foxmail.com

1. J. Luo, Y.-J. Cheng, T.-D. Kim, S. Hau, S.-H. Jang, Z. Shi, X.-H. Zhou and A. K. Y. Jen, *Org. Lett.*, 2006, **8**, 1387-1390.
2. Y. Q. Shi, C. Zhang, H. Zhang, J. H. Bechtel, L. R. Dalton, B. H. Robinson and W. H. Steier, *Science*, 2000, **288**, 119-122.
3. S.-K. Kim, Y.-C. Hung, B.-J. Seo, K. Geary, W. Yuan, B. Bortnik, H. R. Fetterman, C. Wang, W. H. Steier and C. Zhang, *Appl. Phys. Lett.*, 2005, **87**, 061112.
4. L. R. Dalton, P. A. Sullivan and D. H. Bale, *Chem. Rev.*, 2010, **110**, 25-55.
5. L. R. Dalton, D. Lao, B. C. Olbricht, S. Benight, D. H. Bale, J. A. Davies, T. Ewy, S. R. Hammond and P. A. Sullivan, *Opt. Mater.*, 2010, **32**, 658-668.

6. P. A. Sullivan and L. R. Dalton, *Acc. Chem. Res.*, 2010, **43**, 10-18.
7. S. R. Marder, B. Kippelen, A. K. Y. Jen and N. Peyghambarian, *Nature*, 1997, **388**, 845-851.
8. M. Q. He, T. M. Leslie, J. A. Sinicropi, S. M. Garner and L. D. Reed, *Chem. Mater.*, 2002, **14**, 4669-4675.
9. L. Dalton and S. Benight, *Polymers*, 2011, **3**, 1325-1351.
10. P. A. Sullivan, A. J. P. Akelaitis, S. K. Lee, G. McGrew, S. K. Lee, D. H. Choi and L. R. Dalton, *Chem. Mater.*, 2006, **18**, 344-351.
11. Y. Liao, S. Bhattacharjee, K. A. Firestone, B. E. Eichinger, R. Paranjli, C. A. Anderson, B. H. Robinson, P. J. Reid and L. R. Dalton, *J. Am. Chem. Soc.*, 2006, **128**, 6847-6853.
12. F. Dumur, C. R. Mayer, E. Dumas, F. Miomandre, M. Frigoli and F. Secheresse, *Org. Lett.*, 2008, **10**, 321-324.
13. L. R. Dalton, A. W. Harper and B. H. Robinson, *Proceedings of the National Academy of Sciences of the United States of America*, 1997, **94**, 4842-4847.
14. D. Yu, A. Gharavi and L. Yu, *J. Am. Chem. Soc.*, 1995, **117**, 11680-11686.
15. S. R. Hammond, J. Sinness, S. Dubbury, K. A. Firestone, J. B. Benedict, Z. Wawrzak, O. Clot, P. J. Reid and L. R. Dalton, *J. Mater. Chem.*, 2012, **22**, 6752.
16. J. Luo, S. Huang, Y.-J. Cheng, T.-D. Kim, Z. Shi, X.-H. Zhou and A. K. Y. Jen, *Org. Lett.*, 2007, **9**, 4471-4474.
17. I. T. Choi, M. J. Ju, S. H. Song, S. G. Kim, D. W. Cho, C. Im and H. K. Kim, *Chemistry-a European Journal*, 2013, **19**, 15545-15555.
18. Y. Yang, F. Liu, H. Wang, S. Bo, J. Liu, L. Qiu, Z. Zhen and X. Liu, *Journal of Materials Chemistry C*, 2015, **3**, 5297-5306.
19. Y. Yang, H. Xu, F. Liu, H. Wang, G. Deng, P. Si, H. Huang, S. Bo, J. Liu, L. Qiu, Z. Zhen and X. Liu, *Journal of Materials Chemistry C*, 2014, **2**, 5124-5132.
20. R. M. Dickson and A. D. Becke, *J. Chem. Phys.*, 1993, **99**, 3898-3905.
21. M. J. Frisch, G. W. Trucks, H. B. Schlegel, G. E. Scuseria, M. A. Robb, J. R. Cheeseman, G. Scalmani, V. Barone, B. Mennucci, G. A. Petersson, H. Nakatsuji, M. Caricato, X. Li, H. P. Hratchian, A. F. Izmaylov, J. Bloino, G. Zheng, J. L. Sonnenberg, M. Hada, M. Ehara, K. Toyota, R. Fukuda, J. Hasegawa, M. Ishida, T. Nakajima, Y. Honda, O. Kitao, H. Nakai, T. Vreven, J. A. Montgomery Jr., J. E. Peralta, F. Ogliaro, M. J. Bearpark, J. Heyd, E. N. Brothers, K. N. Kudin, V. N. Staroverov, R. Kobayashi, J. Normand, K. Raghavachari, A. P. Rendell, J. C. Burant, S. S. Iyengar, J. Tomasi, M. Cossi, N. Rega, N. J. Millam, M. Klene, J. E. Knox, J. B. Cross, V. Bakken, C. Adamo, J. Jaramillo, R. Gomperts, R. E. Stratmann, O. Yazyev, A. J. Austin, R. Cammi, C. Pomelli, J. W. Ochterski, R. L. Martin, K. Morokuma, V. G. Zakrzewski, G. A. Voth, P. Salvador, J. J. Dannenberg, S. Dapprich, A. D. Daniels, O. Farkas, J. B. Foresman, J. V. Ortiz, J. Cioslowski and D. J. Fox, Gaussian, Inc., Wallingford, CT, USA, 2009.
22. C. Lee and R. G. Parr, *Physical Review A*, 1990, **42**, 193-200.
23. X. Ma, F. Ma, Z. Zhao, N. Song and J. Zhang, *J. Mater. Chem.*, 2010, **20**, 2369.
24. R. V. Solomon, P. Veerapandian, S. A. Vedha and P. Venuvanalingam, *J. Phys. Chem. A*, 2012, **116**, 4667-4677.
25. R. M. El-Shishtawy, F. Borbone, Z. M. Al-Amshany, A. Tuzi, A. Barsella, A. M. Asiri and A. Roviello, *Dyes and Pigments*, 2013, **96**, 45-51.
26. J. Y. Wu, J. L. Liu, T. T. Zhou, S. H. Bo, L. Qiu, Z. Zhen and X. H. Liu, *Rsc Advances*, 2012, **2**, 1416-1423.
27. K. S. Thanthiriwatte and K. M. N. de Silva, *Journal of Molecular Structure-Theochem*, 2002, **617**, 169-175.
28. T. Lu and F. Chen, *J. Comput. Chem.*, 2012, **33**, 580-592.
29. C. C. Teng and H. T. Man, *Appl. Phys. Lett.*, 1990, **56**, 1734.
30. W. B. Wu, J. G. Qin and Z. Li, *Polymer*, 2013, **54**, 4351-4382.
31. Z. a. Li, Z. Li, C. a. Di, Z. Zhu, Q. Li, Q. Zeng, K. Zhang, Y. Liu, C. Ye and J. Qin, *Macromolecules*, 2006, **39**, 6951-6961.
32. Z. Li, Q. Q. Li and J. G. Qin, *Polymer Chemistry*, 2011, **2**, 2723-2740.
33. Z. a. Li, W. Wu, Q. Li, G. Yu, L. Xiao, Y. Liu, C. Ye, J. Qin and Z. Li, *Angew. Chem. Int. Ed.*, 2010, **49**, 2763-2767.
34. W. Wu, R. Tang, Q. Li and Z. Li, *Chem. Soc. Rev.*, 2015, DOI: 10.1039/C4CS00224E.
35. M. Q. He, T. M. Leslie and J. A. Sinicropi, *Chem. Mater.*, 2002, **14**, 2393-2400.
36. J. Wu, C. Peng, H. Xiao, S. Bo, L. Qiu, Z. Zhen and X. Liu, *Dyes and Pigments*, 2014, **104**, 15-23.
37. J. Wu, H. Xiao, L. Qiu, Z. Zhen, X. Liu and S. Bo, *Rsc Advances*, 2014, **4**, 49737-49744.

